

Voltage Control in Distribution Feeders with High Penetration of Wind Energy

JO Petinrin^{1*}, Mohamed Shaaban², MO Petinrin³

¹Electrical and Electronic Department, School of Engineering, Federal Polytechnic Ede, Ede, Osun State, Nigeria

²Department of Electrical Engineering, Faculty of Engineering Port Said University, Egypt

³Department of Mechanical Engineering, Faculty of Engineering Technology, University of Ibadan, Nigeria

Abstract: The recent drift towards balancing generation and consumption, along with increasing demands of high power quality and reliability, require the deployment of energy storage and application of demand response in the smart grid. The potential for using energy storage and demand response promise to have a major impact on schemes for voltage control in a smart grid. This paper presents a comprehensive optimisation architecture that do not only take into consideration the coordination of VAr control devices, but also manages storage facilities and demand response in an hourly operation fashion. An integrated framework on hybrid Particle Swarm Optimisation/Gravitational Search Algorithm (PSOGSA) is used for VAr control devices, energy storage and demand response optimisation scheduling. The effectiveness of the proposed method is validated through a quasi-time sequence analysis over a 24-hourly simulation period. Test results show that the smart coordinated operation among the control devices causes reduction in system losses and enhances system capability to maintain voltages within the prescribed bounds.

Keywords: Demand response, Elastic load, Energy loss, Energy storage, Load tap changer, PSOGSA, Renewable generation, Real-time pricing, Smart grid, Voltage deviation.

I. INTRODUCTION

The problem of global warming and exhaustion of fossil fuel have fostered the increased usage of less environmental-polluting distributed generation (DG) sources closer to load demands in the distribution system (DS). Renewable generations (RGs) integrated in a smart grid (SG) system have undeniably brought forward some positive impacts as far as sustainable energy development is concerned as it retains serious drawbacks [1-3]. In particular, the inability of RG to guarantee continuous energy supply, due to their intermittent and fluctuating nature, is the most imminent one. Non-dispatchable RGs, such as solar and wind energies may not always be available when and where needed [4].

Smart grid concerns the modernization and automation of the power delivery system that seamlessly integrate RGs into the DS with high proportions; no matter where they are sited. However, this may cause grid voltage rise due to the significant amount of active power injection from the RGs and the uncoordinated operation of voltage regulating devices [5]. Therefore, voltage regulation is essential in the DS, if a suitable voltage level at the customer's point of common coupling (PCC) is to be maintained within boundaries. Load tap changers (LTCs) are used for voltage regulation in convectional DS and capacitors which are used as reactive power support to minimize feeder voltage drop [6]. However, LTCs are mechanical devices with delay time between 30 and 60 seconds, therefore, cannot solve the fast intermittent voltage problem caused by RG [7]. Deployment of energy storage (ES) throughout the grid from generation to end-user present an opportunity to transcend the power balance paradigm by storing energy during off-peak, with less line losses, and redispatching this energy when needed [8]. Demand response (DR) is one of smart grid tools that empowers customers and provides them with opportunity to interact with utilities.

Various approaches have been developed in literature to solve the problem of voltage deviation in SG. In [9], dynamic

International Journal of Innovative Research in Science, Engineering and Technology

(An ISO 3297: 2007 Certified Organization)

Vol. 6, Issue 7, July 2017

programming to dispatch on-load tap changer (OLTC) and capacitors based on forecasted hourly loads in a DS is proposed. The optimisation problem of the OLTC and capacitors dispatch was formulated mathematically. Constraints considered are maximum permissible number of switching operations and statutory voltage limits on the DS. Its dynamic programming has relatively small searching space which made the computation burden acceptable. However, large search space is required for optimisation of more VAR control devices, this may be computationally time consuming.

To reduce the computational burden, Jeong [10] proposed dynamic programming, voltage sensitivity and branch-and-bound methods for optimisation of OLTC, SCs and AVR of DGs. The optimisation problem of the OLTC and capacitors dispatch was formulated mathematically as well. The possible steps were limited to 24 stages by employing a flexible search space at each step so as to avoid computational burden. Liu et al. [11] reduced the computational burden on optimal scheduling of VAR control devices by decomposing the whole control through the coordination of dynamic programming method for the substation and fuzzy logic control method for the feeder level. Although the studies in [9,10] have obtained quite promising results on VAR control problem. However, the studies are limited to only OLTC and capacitors without considering SVRs along the feeder lines. Alam [12], proposed distributed energy storage (DES) to mitigate voltage rise problem caused by solar PV in a DS. The method employed enable DES to absorb excess energy at noon day to mitigate the reverse power flow as a result of high PV output. The stored energy is then discharged to support the voltage in the evening peak period. The method considered an over-simplified charge/discharge ES cycle with the assumption of no voltage problem except noon day and evening peak period. However, a preventive control frame work is required to continuously monitor current and voltage at the PCC to establish a real-time equivalent circuit of the DS. This will guide against any changes in load pattern, most especially during holidays, or else application of such model might be detrimental for the DS.

In [13], a coordinated control of LTC and ES for voltage rise mitigation under high PV penetration is presented. The objective of the coordination control is to reduce the LTC operation stress, minimize energy loss and improve voltage profile. However, the VAR control devices does not include capacitor banks and DR is not considered in the study as well as optimisation of the LTCs. Schroede et al. [14] described ES and DR as essential tools in operation of DS and that ES and DR are of good benefit to the system operation by preventing capacity shortage. The authors presented that ES can prevent grid reinforcement at some voltage level without affecting the system security while the DR is even stronger in the presence of flexible demand such as electric vehicles. However, both ES and DR are not optimized and coordinated with VAR control devices. Optimal sizing and siting of the ES is necessary to improve the voltage profile in the DS and reduce losses. Different methods have been employed in the literature for optimal sizing and siting of ES/DG to mitigate the problems associated with uncertainties of RG. Gravitational search algorithm (GSA) and particles warm optimisation-gravitational search algorithm (PSOGSA) are used to determine multiple DG capacity and location in DS in [15] and [16] respectively. An OPF-based algorithm for siting the aggregated capacity of ES was developed to decrease the wind energy curtailment and cost of energy supply in [17]. However, none of the reviewers above employed the hybrid PSOGSA for their search technique on energy storage.

In [18], a novel voltage sensitivity matrix based on voltage sensitivity analysis is proposed. The voltage sensitivity is due to customers' load participation in DR program. The result shows that load curtailment reduces voltage drop across the DS and improve voltage profile. However, the cost of incentives to participating customers are not considered.

The effect of incentive-based DR on distribution system voltage profile was carried out in [19]. A demand-price elasticity matrix was modelled for participating customers. However, the model lacks the control option to carry out the incentive -based DR program. In [20], a power network where customers manage their electricity usage by playing games among one another in response to utility 24-hour electricity price scheduling is proposed. Due to customers' participation in dynamic pricing, there is improvement in voltage profile and the cost of energy is reduced while keeping customers' satisfaction at a high level. However, the proposed algorithm required customers to update their energy usage scheduling asynchronously with the assumption that

International Journal of Innovative Research in Science, Engineering and Technology

(An ISO 3297: 2007 Certified Organization)

Vol. 6, Issue 7, July 2017

each customer has full information of generation cost function. This proposal is hard to realize in practice. Zhao [21] set up a general architecture of energy management system (EMS) in a home area network. With the application of the EMS in the home, the authors then presented a GA in scheduling the electricity consumption in the home so as to minimize energy cost and peak-average-ratio. Consumers energy cost is reduced by changing elastic loads in response to utility declared price and the system voltage profile is improved.

The author in [22] had proposed a voltage control scheme that coordinates the VVAr control devices along with energy storage to mitigate integration issues associated with wind generation. The proposed voltage control scheme is formulated in this paper as a nonlinear programming problem to minimize voltage deviations and power losses. A hybrid Particle Swarm Optimization-Gravitational Search Algorithm (PSOGSA) is used to solve the resulting optimization problem. The PSOGSA combined the social thinking ability in particle swarm optimization (PSO) with the gravitational search algorithm (GSA) local search skill. They are robust, able to perform multi-directional search and determine near global optimization solutions. Test results confirm the effectiveness the energy storage together with the coordination of the VVAr devices to maintain the system voltage within the prescribed limits. However, DR is not considered. This paper presents a comprehensive optimisation architecture that do not only take into consideration the coordination of VAr control devices, but also manages ES facilities and DR in an hourly operation fashion. This gives the utility company options in selecting appropriate and effective voltage control measures. The developed framework is amenable to incorporate additional market instruments or SG tools that can enhance integrity of the system operation. The paper also developed an extensive multiperiod modeling approach using quasi-time sequence analysis, based on Open distributed system simulator (OpenDSS) with Matlab interface, for the voltage control problem in distribution networks (DNs) with high penetration levels of wind energy.

II. OPTIMISATION OF VAR CONTROL DEVICES, ENERGY STORAGE AND DEMAND RESPONSE

The main function of coordinating VAr control devices, such as LTC transformers and switched capacitors; ES and DR in modern smart DN is to offset the impact of intermittency introduced by connecting variable RG to the system at the PCC. More blatantly, it is required to employ the VAr devices along with ES and DR to minimize the overall losses and support the system voltage profile. Therefore, the problem of optimising VAr control devices, ES and DR can be cast a multiperiod optimisation problem, where the objective is to minimize hourly energy losses and voltage deviations across various network nodes. This can be expressed mathematically as [23]:

$$\text{Min } F = w_v \sum_{i=1}^N \sum_{t=1}^T \|V_{i,t} - V_{ref}\|^2 + w_l \sum_{i=1}^N \sum_{t=1}^T P_{Li,t} * \Delta t \quad (1)$$

Where, w_v and w_l are the weighted-coefficients of voltage minimization and loss minimization respectively. $V_{i,t}$ and V_{ref} are the voltage of bus i at time t and magnitude of voltage reference respectively, obtained from the distribution power flow. $P_{L,t}$ is the network loss at time t . T is the number of time in hour, Δt is 1 hour time interval and N is the number of buses.

The sum of the total power losses including the energy storage is contemplated as [24]:

$$P_{Li,t} = \sum_{j=1}^N [\alpha_{ij,t} (P_{i,t} P_{j,t} + Q_{i,t} Q_{j,t}) + \beta_{ij,t} (Q_{i,t} P_{j,t} + P_{i,t} Q_{j,t})] \quad i \in N \quad (2)$$

Where, $\alpha_{ij,t} = \frac{r_{ij}}{V_{i,t} V_{j,t}} \cos(\delta_{i,t} - \delta_{j,t})$,

$$\beta_{ij,t} = \frac{r_{ij}}{V_{i,t} V_{j,t}} \sin(\delta_{i,t} - \delta_{j,t})$$

$Z_{ij} = r_{ij} + x_{ij}$ is the ij th element of $[Zbus]$ matrix

$P_{i,t} = P_{Gi,t} - P_{Di,t} \pm P_{ESi,t}$, $Q_{i,t} = Q_{Gi,t} - Q_{Di,t} \pm Q_{ESi,t}$.

International Journal of Innovative Research in Science, Engineering and Technology

(An ISO 3297: 2007 Certified Organization)

Vol. 6, Issue 7, July 2017

$P_{i,t}$ and $Q_{i,t}$ are the net active and reactive power injection at bus i at time t , $P_{Gi,t}$ and $Q_{Gi,t}$ are the active and reactive powers generated from the variable renewable generation at time t . $P_{ESi,t}$ and $Q_{ESi,t}$ are the active and reactive power produced/absorbed by the energy storage at bus i at time t , while $P_{Di,t}$ and $Q_{Di,t}$ are the load active and reactive powers at bus i at time t respectively.

The constraints include the power balance equality constraints which can be represented as:

$$P_{i,t} = V_{i,t} \sum_{j=1}^N V_{j,t} [G_{i,j} \cos(\delta_{i,t} - \delta_{j,t}) + B_{i,j} \sin(\delta_{i,t} - \delta_{j,t})] \quad (3)$$

$$Q_{i,t} = V_{i,t} \sum_{j=1}^N V_{j,t} [G_{i,j} \sin(\delta_{i,t} - \delta_{j,t}) - B_{i,j} \cos(\delta_{i,t} - \delta_{j,t})] \quad (4)$$

Where, $V_{i,t}$ is the voltage at bus i at time t , $G_{i,j}$ and $B_{i,j}$ are the conductance and susceptance of the line between buses i and j respectively, whereas $\delta_{i,t}$ is the voltage angle at bus i at time t .

Voltage constraints:

$$V_{\min,t} \leq V_i \leq V_{\max,t} \quad i \in N \quad (5)$$

Other constraints to be considered for optimal scheduling of LTC transformers and switched capacitors for the objective function are:

Maximum Switching Operation of LTC

$$\sum_{t=1}^{24} |T_t - T_{t-1}| \leq K_T \quad (6)$$

$$T_{\min,t} \leq T_t \leq T_{\max,t} \quad (7)$$

$$[V_S]_{abc,t} = [n_R]_{abc,t} [V_R]_{abc,t} \quad (8)$$

$$n_R = 1 \pm T_t \Delta V_t \quad (9)$$

Maximum Switching Operation of Switched Capacitors

$$\sum_{t=1}^{24} (C_{cct} \oplus C_{cct-1}) \leq K_C; \quad c = 1, 2, \dots, nc \quad (10)$$

$$Q_{i,t} = \omega C V_{i,t}^2 \quad (11)$$

$$Q_{\min,t} \leq Q_{i,t} \leq Q_{\max,t} \quad (12)$$

Where V_{\min} and V_{\max} are minimum and maximum voltage limits at bus i respectively, k_T and T_t are the allowed maximum LTC switching and LTC tap position at time t respectively. k_C and C_{cct} are the allowed maximum capacitor switching and status of capacitor at time t respectively. V_S and V_R are the regulator input and output voltage respectively, ΔV_t (0.00625) is tap change step and n_R is the effective turn's ratio of the regulator. The number of installed capacitor is nc . \oplus is logic operator XOR (exclusive OR) that returns "1" if C_{cct} is not equal to C_{cct-1} and returns "0" if C_{cct} is equal to C_{cct-1} . C_{cct} and C_{cct-1} are the states of capacitor c at hour t and $t-1$ respectively.

Other constraints to be considered for optimal siting and sizing of energy storage for the objective function are:

Storage Physical and Operating Limits

$$P_{i,t} = P_{Gi,t} - P_{Di,t} \pm P_{ESm,t} \quad m \in M, \quad M \subseteq N \quad (13)$$

International Journal of Innovative Research in Science, Engineering and Technology

(An ISO 3297: 2007 Certified Organization)

Vol. 6, Issue 7, July 2017

$$\sum_{t=1}^{24} P_{ES_{i,t}} \Delta t \eta_i \leq E_{ES_{i,t}}^0 \quad (14)$$

$$\sum_{t=1}^{24} -P_{ES_{i,t}} \Delta t \eta_i \leq E_{ES_i}^{\max} - E_{ES_i}^0 \quad (15)$$

$$E_{ES_{m,t}}^{\min} \leq E_{ES_{m,t}} \leq E_{ES_{m,t}}^{\max} \quad (16)$$

$$P_{ES_{m,t}}^{\min} \leq P_{ES_{m,t}} \leq P_{ES_{m,t}}^{\max} \quad (17)$$

$$\left(P_{ES_{m,t}}\right)^2 + \left(Q_{ES_{m,t}}\right)^2 \leq \left(C_{ES_{m,t}}^{\max}\right)^2 \quad (18)$$

Where η is the energy storage charge-discharge cycle efficiency, E_{ES} is the energy stored in the energy storage, and $E_{ES_i}^0$ initial energy stored at bus i and time t . E_{max} and E_{min} is the maximum and minimum capacity of the energy storage respectively. C_{max} is the power capability limit of the energy storage and M is the number of storage elements.

Power loss constraint:

$$P_{Li,t}^{with ES} \leq P_{Li,t}^{without ES} \quad (19)$$

where $P_{Li,t}^{with ES}$ and $P_{Li,t}^{without ES}$ are the power loss with and without energy storage.

Equations (14) and (15) respectively denote the maximum and minimum amount of the energy stored or discharged from the energy storage. Similarly, (16) and (17) are the maximum and minimum energy storage capacity respectively with the relevant active power rating. Based on the assumption that the energy storage is interfaced with the distribution network through efficient power electronic converters, Eq. (18) models the capability curve of the energy storage.

The formulation from (13) to (19) gives a complete mathematical programming description for the modelling of energy storage necessary to counterbalance the impact of the variable renewable energy on system losses and voltage profile.

Demand Response Operating Limits

$$P_{i,t} = P_{RG_{i,t}} - P_{D_{i,t}} \quad \forall t \in T \quad (20)$$

$$P_{D_{i,t}} = P_{U_t} + P_{E_t} \quad \forall t \in T \quad (21)$$

$P_{D_{i,t}}$ is a process that satisfy

$$P_{D_{i,t}}^{\min} \leq P_{D_{i,t}} \leq P_{D_{i,t}}^{\max} \quad \forall t \in T \quad (22)$$

Where $P_{D_{i,t}}$ is total power usage, P_{U_t} and P_{E_t} are the inelastic and elastic load at time t respectively.

The elastic loads are divided into controllable and shifted loads. Controllable loads are thermostatically controlled loads such as heating and ventilating loads, whereas shifted loads are load that can be shifted to another time such as electric vehicle, washing machines etc. Inelastic loads are loads that can neither be shifted nor controlled such as lighting loads.

$$P_{E_t} = P_{C_t} + P_{S_t} \quad (23)$$

Each customer operates a set of A_b appliances. For each appliance $a \in A_b$, the power drawn at time $t \in T$ is denoted as $P_{a,t}$, and by P_a the vector $(P_{a,t}, t \in T)$ representing the total power for the day.

International Journal of Innovative Research in Science, Engineering and Technology

(An ISO 3297: 2007 Certified Organization)

Vol. 6, Issue 7, July 2017

$$P_{C_t} = \sum_a P_{a_t} \quad \forall t \in T \quad (24)$$

$$P_{S_t} = \sum_a \sum_{t'} P_{S_{t't}^a} - \sum_a \sum_{t'} P_{S_{t't'}^a} \quad \forall t \in T \quad (25)$$

$$0 \leq \sum_a P_{S_{t't}^a} \leq B \times P_{a_t} \quad \forall a \in A, \forall t \in T \quad (26)$$

$$P_{S_{t't'}^a} = 0, \forall a \in A_b, \forall t' \in T \quad (27)$$

Where P_{C_t} and P_{S_t} are the controllable load at time t and load shifted to time t respectively. P_{a_t} is power of appliances a at time t , $P_{S_{t't}^a}$ is power of appliance a that is shifted from time t to time t' and B is number of DR participating customers.

The optimal solution of customers using real-time pricing (RTP) depends on the declared retailer price $\lambda_t := (\lambda_t, t \in T)$ so as to encourage customers to participate in RTP schedule. The product of price (λ_t) and the real-time power usage (P_{D_t}) is the payment or total price ($\lambda_i(t)$) paid by customer to the retailer.

$$\lambda_i(t) := \lambda_t(P_{D_t}, t) \quad \forall t \in T.$$

$$\lambda_i(t) = \bar{\lambda}_t(P_{U_t}) + \hat{\lambda}_t(P_{E_t}) \quad \forall t \in T \quad (28)$$

$$\hat{\lambda}_t < \bar{\lambda}_t, \quad \forall t \in T \quad (29)$$

$$\bar{\lambda} \sum_{t=1}^T P_{u_{k,t}} + \sum_{t=1}^T P_{E_{k,t}} \hat{\lambda}_t < \bar{\lambda} \sum_{t=1}^T (P_{u_{k,t}} + P_{E_{k,t}}) \quad (30)$$

Where, $\lambda_i(t)$, $\hat{\lambda}_t$ and $\bar{\lambda}_t$ are the total price, real-time price and flat rate price at time t respectively.

Power Loss Constraint for DR

$$P_{Li,t}^{with DR} \leq P_{Li,t}^{without DR} \quad (31)$$

Where, $P_{Li,t}^{with DR}$ and $P_{Li,t}^{without DR}$ are the power loss with and without demand response.

Equation (21) denotes new hourly load profile as a result of elastic load and (24) described total available controllable load. The net load shifted to hour t is expressed in (25), (26) caps the total shifted elastic load at the respective time and (27) insure that the operation time of elastic loads is not displaced to an earlier time. The formulation from (20) to (31) gives a complete description for the modelling of demand response necessary to counterbalance the impact of the variable renewable generation on system losses and voltage profile.

Weighting Factor

To avoid multiobjective programming and generate an equivalent single-objective optimisation problem, a non-inferior-solution method is developed to assign weights to the various objective functions [25]. Each objective function is multiplied by scalar coefficients called weighting factors. The weighting factors are usually normalized as:

$$\sum_{k=1}^K W_k = 1 \quad (32)$$

Therefore, $w_v + w_1 = 1$.

International Journal of Innovative Research in Science, Engineering and Technology

(An ISO 3297: 2007 Certified Organization)

Vol. 6, Issue 7, July 2017

The convergence criterion of the maximum number of generation is checked after the fitness of each individual in a population is evaluated by the following fitness function.

$$Fitness = \left[w_v \sum_{t=1}^T \sum_{i=1}^N (V_{i,t} - V_{ref})^2 + w_L \sum_{t=1}^T \sum_{i=1}^N P_{L_{i,t}} \right] \quad (33)$$

III. HYBRID PARTICLE SWARM OPTIMISATION - GRAVITATIONAL SEARCH ALGORITHM (PSOGSA)

This paper employed hybrid PSOGSA, a combination of particle swarm optimisation (PSO) and GSA low-level co-evolutionary heterogeneous hybrid. The combination of the functionality of both PSO and GSA makes it to be low-level and it is co-evolutionary because both PSO and GSA algorithms are use one after another. PSOGSA is heterogeneous because the two algorithm are combine together to produce final result [26]. The hybrid PSOGSA combined the social thinking ability in PSO with the GSA local search skill. The equation for the combined algorithm is as in [26]:

$$vel_i(t+1) = \omega vel_i(t) + C_1 rand(a_i(t)) + C_2 rand(Gbest - s_i(t)) \quad (34)$$

Where vel_i is velocity on agent i , ω is weighting function, $a_i(t)$ acceleration on agent i at time t . C_1 and C_2 are constants, s_i and s_j are position of agent i and agent j respectively and Gbest is global best solution.

The particle position is updated in each iteration as:

$$s_i(t+1) = vel_i(t+1) + s_i(t) \quad (35)$$

Fitness value is evaluated to determine the quality of solution for procedure updating. Other agents which are exploring the search space are attracted by agents which are closer to the good solution. All the agents move very slowly when they are closer to a good solution. At this point, Gbest assists the agents to exploit the global best. Then, the best solution found so far is saved in the memory (Gbest) by PSOGSA for each agent's accessibility at any time as they tend toward it. The capability of local and global search can be balanced by adjusting C_1 and C_2 .

The optimisation procedure using POSGA is as follows:

Agent's Initialization

Initialize the positions of the N number of agents randomly as:

$$s_i = (s_i^1, \dots, s_i^d, \dots, s_i^n), \text{ for } i = 1, 2, \dots, N \quad (36)$$

Where s_i^d is the positions of the i^{th} agent in the d^{th} dimension and n is the space dimension.

Fitness Evaluation

Fitness function is the driving force in POSGA which is used to evaluate each particle for quality of solution in the initial population. Any violation of constraints attracts a penalty of 1.0.

Parameters Computation

Gravitational forces and resultant force among agents are computed using (37) to (38).

After which the particle's acceleration are determined using (39).

Gravitational force

International Journal of Innovative Research in Science, Engineering and Technology

(An ISO 3297: 2007 Certified Organization)

Vol. 6, Issue 7, July 2017

$$F_{ij}^d(t) = G(t) \frac{M_{pi}(t)M_{aj}(t)}{R_{ij}(t) + \tau} (s_j^d(t) - s_i^d(t)) \quad (37)$$

$$\text{Where, } G(t) = G_o \exp(-\gamma t \text{re} / \text{I}t\text{re}_{\max})$$

The total force acting on agent i in a problem space with dimension d is as:

$$F_i^d(t) = \sum_{j=1, j \neq i}^N \text{rand} F_{ij}^d(t) \quad (38)$$

Acceleration of all agents is given as:

$$a_i^d(t) = \frac{F_i^d(t)}{M_i(t)} \quad (39)$$

Where $F_{ij}^d(t)$ is gravitational forces from agent j on agent i at time t , $F_i^d(t)$ is gravitational forces on agent i at time t , $G(t)$ is gravitational constant at time t and G_o is initial gravitational force value. $\text{I}t\text{er}$ and $\text{I}t\text{er}_{\max}$ are current and maximum iteration and γ is descending coefficient to control gravitational constant decay rate. M_{pi} and M_{ai} are passive and active gravitational mass related to agent j and agent i respectively and M_i is mass of object. $R_{ij}(t)$ is the Euclidan distance between two agents i and j , N is number of solution, τ is small constant, d is dimension of problem space, and rand is random number in the interval $[0, 1]$. Initial mass of the particle is updated with the following formulas:

$$M_{ai} = M_{pi} = M_{ii} = M_i, (i = 1, 2, 3, \dots, N) \quad (40)$$

$$m_i(t) = \frac{\text{fit}_i(t) - \text{worst}(t)}{\text{best}(t) - \text{worst}(t)} \quad (41)$$

$$M_i(t) = \frac{m_i(t)}{\sum_{j=1}^N m_j(t)} \quad (42)$$

Where, $\text{fit}(t)$ is the fitness value of particles.

Best (t) and worst (t) are determined as:

$$\text{best}(t) = \min_{j \in (1, \dots, N)} \text{fit}_j(t) \quad (43)$$

$$\text{worst}(t) = \max_{j \in (1, \dots, N)} \text{fit}_j(t) \quad (44)$$

Velocity and Position Updates

Determine the velocity and position of all agents at the next iteration using (37) and (38) respectively and update them with new calculations.

Repetition:

Repeat the above procedures until maximum iteration limit is reached.

The best fitness value is computed at the final iteration while the corresponding agent position at specified dimensions is calculated as the global solution. A developed code using PSOGA toolbox package implemented in Matlab environment is used in the optimization. Fig. 1 depicts the flowchart of PSO GSA. The parameter used is illustrated in Table 1 and results are obtained after several simulations.

Penalty function is introduced to handle constraints (particularly, inequality constraints) in the optimisation. This converts a constrained optimisation problem into an unconstrained one by adding 1 to the objective function based on the total number of

International Journal of Innovative Research in Science, Engineering and Technology

(An ISO 3297: 2007 Certified Organization)

Vol. 6, Issue 7, July 2017

constraint violation found in the solution.

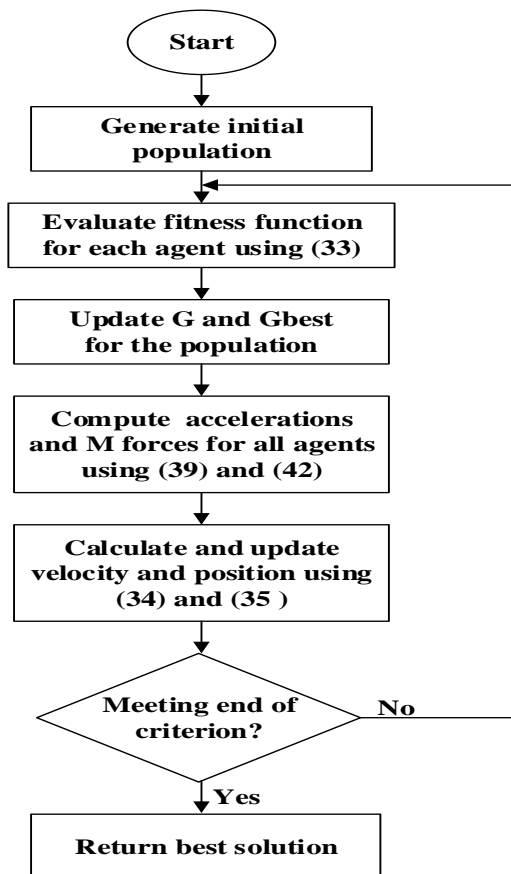


Fig. 1 PSOGSA optimization flowchart.

Table 1. PSOGA parameters.

	Pop size	Iteration	C1	C2	α	G ₀	ω_{\min}	ω_{\max}
GSA	20	100	1	1	20	100	1	1
PSOGSA	20	100	0.5	1.5	23	1	0.4	0.9

IV. TEST RESULTS

The proposed method is carried out on a modelled IEEE 123 bus feeder of an actual 115 kV/4.16 kV. The total load is modified to 16 MW and is distributed among commercial and residential energy consumers.

The weighting factors for the total voltage deviation are chosen with a higher priority than that of power losses. This is because of its important effect on network operation. The weights are chosen as $w_v = 0.55$ and $w_l = 0.45$.

International Journal of Innovative Research in Science, Engineering and Technology

(An ISO 3297: 2007 Certified Organization)

Vol. 6, Issue 7, July 2017

Table 2. Results on sizing and siting of energy storage.

CES				DES			
GSA		PSOGSA		GSA		PSOGSA	
Bus	Size(MW)	Bus	Size (MW)	Bus	Size (MW)	Bus	Size (MW)
81	2.485	81	2.485	81	1.249	81	1.258
				67	0.826	70	0.575
				78	0.243	78	0.270
				90	0.217	43	0.385

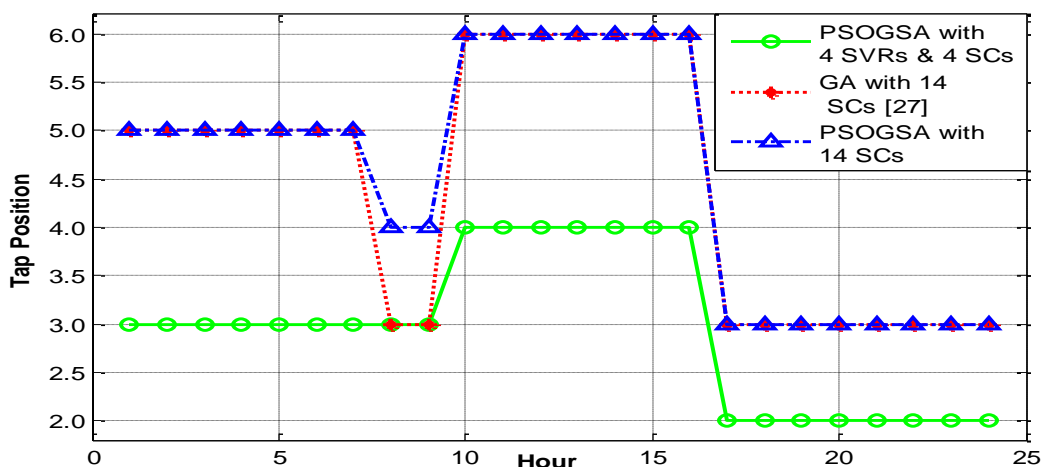


Fig. 2. Comparison between PSO GSA and GA [27] on OLTC operations.

Table 3. Optimal scheduling of OLTC, SVRs and capacitors.

Hour	OLTC	SVR2	SVR3a	SVR3c	SVR4a	SVR4b	SVR4c	SC1	SC2	SC3	SC4
11	4	-2	1	-1	2	1	4	1	1	0	0
12	4	-2	1	-1	2	1	4	1	1	1	0
13	4	-2	1	-1	2	1	4	1	1	1	1
14	4	-2	1	-1	2	1	4	1	1	1	1
15	4	-2	1	-1	1	3	1	1	0	0	1

Table 4. Error analysis of energy storage capacity.

	x ₁	x ₂	x ₃	x ₄	x ₅	x ₆	x ₇	x ₈	x ₉	x ₁₀	$\bar{x} = \frac{1}{n} \sum_{i=1}^n x_i$	$\sigma = \sqrt{\frac{\sum_{i=1}^n (x_i - \bar{x})^2}{n-1}}$
CES	2.485	2.478	2.485	2.488	2.472	2.485	2.488	2.485	2.478	2.485	2.4829	0.0022
DES	1.258	1.258	1.187	1.242	1.258	1.258	1.198	1.258	1.258	1.317	1.2490	0.0359
	0.575	0.575	0.567	0.567	0.580	0.575	0.587	0.575	0.575	0.580	0.5752	0.0060
	0.278	0.270	0.270	0.283	0.267	0.270	0.270	0.283	0.270	0.267	0.2720	0.0062
	0.383	0.383	0.385	0.385	0.388	0.385	0.385	0.380	0.369	0.375	0.3818	0.0057

The proposed method has been implemented in MATLAB, and examined on the test system using OpenDSS Com Matlab interface for a multi-period of 24 hours. The optimal scheduling of LTC and capacitors including the size and location of the ES are determined using the proposed algorithm, described in Fig. 1, are listed in Tables 2 and 3 respectively. Only the results of 11.00 to 15.00 hour are tabulated in Table 3 in order to reduce space. All the capacitors are not switched ON at the same hour except 13.00 hr and 14.00 hr as depicted in the Table 3. This is to compensate for the load demand at the peak hour of the day by injecting more reactive power into the feeder so as to reduce the line losses and improve the voltage profile. The positive number

indicates the regulator tap move up to increase the voltage whereas the negative number points out to the regulator tap move down to reduce the voltage to permissible limits. The proposed algorithm is compared to [27]. We disable the SVRs and connected 14 capacitors in the feeder as it was done by [27]. The comparative results are as shown in Fig. 2. It is observed that there is no significant difference in both algorithms when 14 capacitors are used but the use of SVR in this paper minimizes the OLTC tap operations. It also reduces the number of capacitors and its switching operations. It is clear from the tables that, the proposed PSO-GSA-based approach is capable of determining the optimal scheduling of LTC and capacitors as well as the ES location at a single location or multiple locations with the same size. Error analysis of the ES capacity using PSO-GSA is carried out for the purpose of accuracy. The result of the error analysis is shown in Table 4. Where x is the ES capacity, \bar{x} is mean, σ is standard deviation and n is the number of observations. It is observed in Table 4 that the standard deviation is low which implies a better accuracy of the ES capacity.

Case 1:

Real-time pricing for peak load reduction in a distribution system: Electricity consumption scheduling algorithm that use real-time pricing in a SG environment is carried out. Flat pricing, which is commonly used, is based on long-run average cost. However, retailers depend on bilateral contracts, including wholesale spot market, to purchase the energy they supply to customers. The underlying cost structure is therefore difficult to be estimated. Hence, publicly available wholesale market data as shown in Fig. 3 [28], is used in this paper to estimate the system-level costs incurred by the retailer. Consumers controlled their elastic loads based on the electricity price released by retailer. A load limit $0 \leq P \leq 3850 \text{ kW}$ is set, so that any customer that exceeds the load limit will receive a penalty. That is, making excess payment for the extra load.

The elastic load of respective customers is the controllable load for load reduction or shifting. The feeder consists of 20 kW load, 40 kW load and 75 kW load and above. It is assumed that 20 kW and below is inelastic load, loads above 20 kW to 40 kW are assumed to be controllable loads while any load above 40 kW is assumed to be shifted load. The loads are taken in the proportion of 20%, 50% and 30% for inelastic, controllable and shifted load respectively. Load reduction was applied on the controllable loads while the shifted load is shifted from hour t to t' , that is, from day to night.

A 24-hour consumer's scheduled load curve using the proposed algorithm is as shown in Fig. 4. Every customer managed their load not to exceed the maximum load limits. It is observed that the load profile is dramatically improved. Due to customer's participation in the DR program. The result of the proposed algorithm is compared to price elasticity matrices use in [19]. Both results show that the load reduction/shifting due to the implementation of DR reduced the system line losses causing improvement in the feeder voltage profile. The load reduction and shifting to an off-peak hour effect reduction in the line loss causing boost in the system voltage. In fact, with DR, shifting of load to a more convenient time minimizes the possibility of involuntary emergency load curtailment thereby, diminishes duration of service interruptions. This shows the effectiveness of DR in not only improving the voltage profile during peak-load period but also during off-peak period.

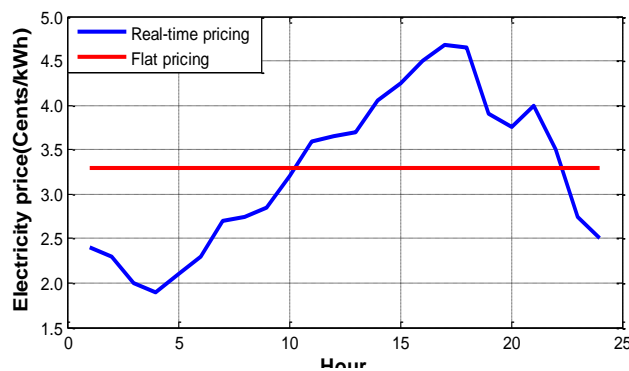


Fig. 3. 24-hour electricity price released by retailer.

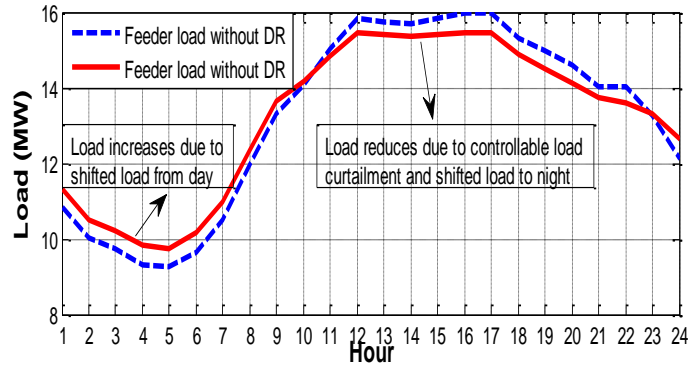


Fig. 4. 24-hour power usage (load) scheduled curve.

Case II:

Effect of energy storage and demand response on system voltage: A 30% wind energy is distributed in the modified peak load feeder of 16 MW. The corresponding voltage profile and system real energy losses are obtained with the optimal settings of LTCs, shunt capacitors and ES/DR through simulation in OpenDSS Com Matlab interface. The LTCs and the capacitor banks are coordinated with the ES and DR for smooth operation to achieve the desired objectives of this paper. Chronological 24-hourly simulation of the system is carried out as shown in Fig. 5. It is observed that the LTCs could not maintain the voltage within statutory limits. Switching ON the capacitor banks increases the voltage profile yet, still below the voltage limits in some hours of the day. The capacitors have great influence on the reactive power flow and line current is reduced, thereby reducing the line voltage drop. The more the capacitor banks are introduced, the more the losses get reduced and the more the voltage profile is improved. A total energy storage of 2.485 MW is distributed in the feeder at their respective optimal locations as determined by the PSO-GSA optimisation. The ES batteries used are divided into two sections because the maximum charging and discharging rate is 6 hours each. The charging trigger is set at 100%. While the discharge trigger is set at 90% so that the battery will not completely discharge before it is re-charged. Section ‘A’ comprises only the ES on bus 81. Section ‘B’ comprises the ES integrated at buses 70, 78 and 43. The charging, discharging and idle hours of each section is shown in Fig. 6. The VAR control devices are coordinated with the ES. The dispatch operation of the ES injects more power into the feeder.

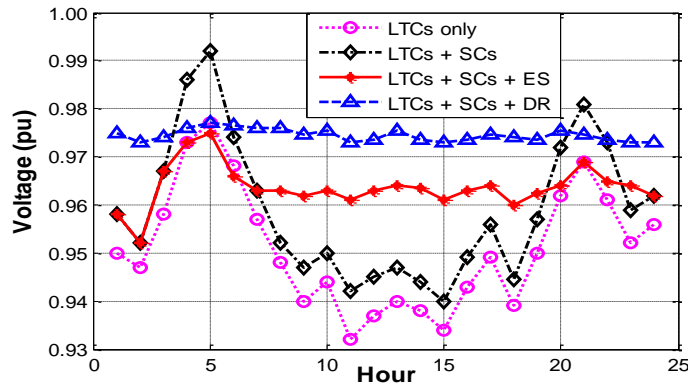


Fig. 5. Application of control devices at different stage.

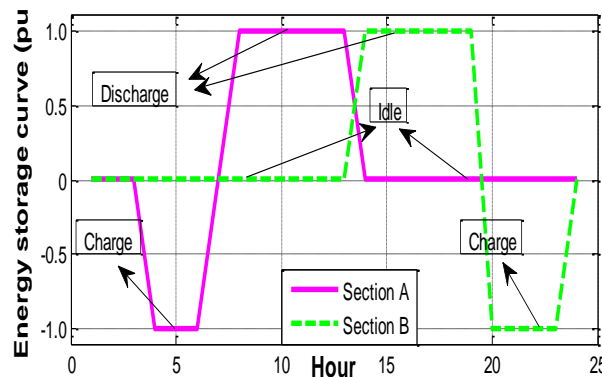


Fig. 6. Energy storage dispatch curve.

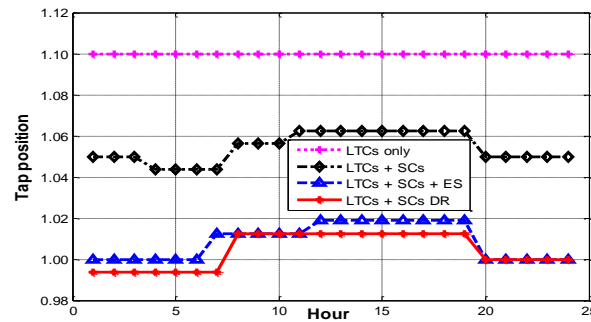
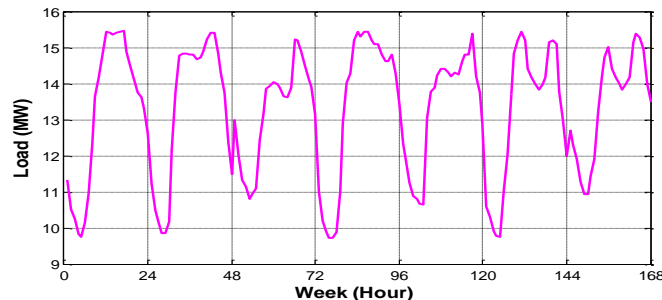
Table 5. Voltage profile, LTCs and losses with and without ES and DR.

	LTCs	SCs	ES	DR
Max Voltage (pu)	0.9772	0.9923	0.9752	0.9771
Min Voltage (pu)	0.9323	0.9405	0.9600	0.9732
Voltage deviation	0.0449	0.0518	0.0152	0.0039
No. of Tap	1	5	3	3
Tap position	16	8 to 10	1 to 3	-1 to +2
Losses (kW)	1779.60	1309.39	1169.39	927.84
(%) Loss Reduction	-	26.42	34.29	47.86

The integration of the ES has warranted voltage profile improvement, energy loss reduction and bring the voltage within statutory limit. For peak-valley levelling of the feeder, the ES is disconnected and real-time pricing DR is introduced. This new measure is coordinated with the VAR control devices. The result is as shown solid line in Fig. 5. The results consistently indicate that the coordinated operation of the VAR control devices with ES and DR causes reduction in system losses and enhances system capability to maintain voltages within the permissible bounds. The use of ES effectively assists to harness intermittent renewable energy resources, reduced energy loss and improve the voltage profile. The use of DR emphasizes its role as a remedy to the voltage depression problem in a smart grid, when the coordination of other control devices fell short in restoring the voltage within its prescribed bounds. It also provides additional flexibility to the system to hedge against the fluctuations of wind energy. The detail of energy loss at the 11th hour of the day with corresponding percentage energy loss reduction is illustrated in Table 5. It is observed that as the ES and DR are introduced, the energy loss reduces and the percentage energy loss reduction increases. This energy loss reduction leads to voltage improvement. The distribution of ES and implementation of DR reduce peak load demand and adapt controllable load to fluctuating wind energy.

Case III:

Effect of VAR control devices, energy storage and DR on load tap changer transformer operation: The LTCs and capacitors are coordinated with the ES and DR so as to reduce energy loss and improve the voltage profile. The LTC '4b' tap operation at different hour of the day is as shown in Fig. 7. The LTC tap moves once without other control devices. However, it moves up to the maximum position, 16 and still could not bring the voltage to the statutory limits. The tap position moves between 8 and 10 with 5 operations when the capacitor banks are switched ON. The integration of the ES made the tap to operate 4 times with the tap position between 1 and 3. However, at the application of DR, the tap position moved 3 times with its position between -1 and 2 to keep to voltage within the permissible limits. This shows that the integration of ES or the use of DR reduce stress on the LTCs as compared to only VAR control devices. Although, the LTC tap moves 3 times within 24 hours with minimum tap position, the coordination of the VAR control devices with either ES or DR bring the voltage profile within the statutory limits.

**Fig. 7.** Regulator tap position at different control levels.**Fig. 8.** Weekly power usage (load) scheduled curve.

Case IV:

Application of DR in peak shaving/load leveling: Wind penetration on the distribution feeder for one week with the application of DR is investigated for peak shaving/load leveling. The feeder load remains the same at 16 MW peak load. However, a weekly power usage curve as shown in Fig. 8 is introduced. Fig. 9 illustrated each day load curve. The VAR control devices are coordinated with the real-time pricing DR. The result is as shown in Fig. 10. Application of DR failed to bring the voltage to permissible bounds on day three as a result of drop in wind generation due to low wind speed. Therefore, energy storage was quickly integrated to inject more power into the feeder so as not to impair customers' welfare. The introduction of the energy storage brings the voltage to permissible bounds. The load output power, wind power and output power of the demand response is illustrated in Fig.11.

Results consistently indicated that the coordinated operation of the VAR control devices with the DR also enhances system capability to maintain voltages within the permissible bounds with the voltage deviation between 0.9502 pu and 0.9615 pu. Energy storage system quickly restore the system to permissible limits when the coordination of VAR control devices with DR failed on the 3rd day. This case study confirm that the developed framework is not only practical and effective for 24-hour time series voltage control analysis but multi-period (long time) voltage control analysis which take into account a sudden drop in wind generation.

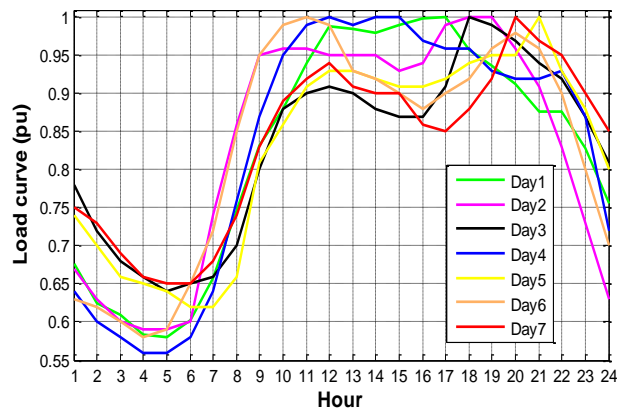


Fig. 9. Daily load curve.

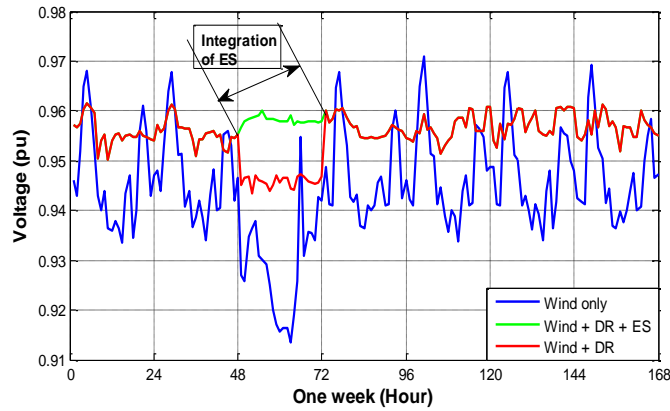


Fig. 10. Weekly voltage profile with and without DR.

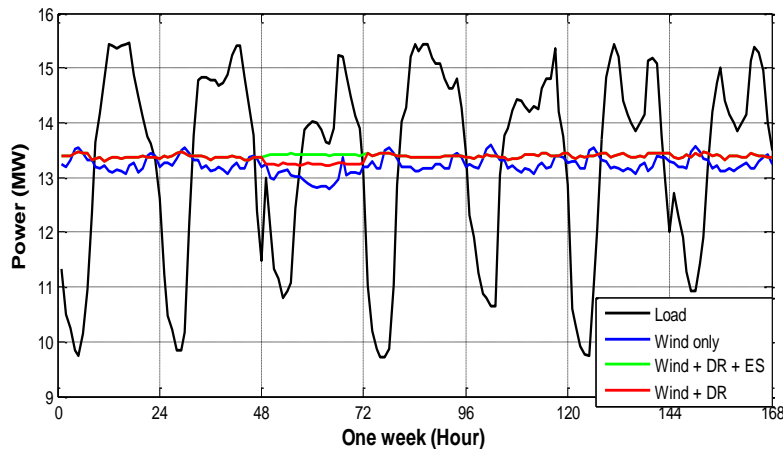


Fig. 11. Weekly power delivered with and without DR.

V. CONCLUSION

High penetration of PV installations and wind farms can potentially cause voltage rise problems. This paper has presented a conjoint framework that incorporates VAr control devices, along with ES and DR to mitigate the voltage variations resulting from deep penetration levels of wind units in DNs. The problem is cast as a mixed-integer, nonlinear optimization problem to minimize voltage deviations and total system losses. Hybrid PSO-GSA is proposed to solve the resulting problem due to its combinatorial nature. The potency of the proposed approach is corroborated through a chronological, multiperiod simulation for 24 hours and is examined under various operating conditions and test scenarios. Results consistently indicate that the coordinated operation of the control devices causes reduction in system losses and enhances system capability to maintain voltages within the permissible bounds.

The use of ES and DR effectively assists to harness intermittent renewable energy resources, and provide additional flexibility to the system to hedge against the fluctuations of variable RG output. The proposed PSO-GSA based optimisation can effectively determine a distributed energy storage locations or centralized energy storage location in distribution feeder. The use of ES, as illustrated in the paper, effectively assist to harness intermittent wind energy resources, mitigate voltage rise resulting from the high penetration of wind energy, bring further improvement to overall voltage profile and accommodate higher penetration levels of wind energy resources. Electrical energy storage distributed in the grid will not only be a key enabler for a smarter distribution feeder with high penetration of wind energy resources but also to provide for reliable and higher quality of power supply.

Aggregate DR that curtails some of the customer load could be hypothetically comparable to the provision of reserves by generators. It thus has the capability to defer future generation investment. DR was explored in this paper as a tool to maintain the voltage profile in a distribution feeder that has a deep penetration of wind energy. The problem of invoking DR options among shiftable and curtailable load portions was modeled as a nonlinear optimization problem. DR techniques, enabled shifting the demand from high electricity price peak period to lower price, off-peak periods. DR can definitely facilitate the integration of higher proportion of renewable generation into the smart grid and alleviate supply pressure on utility companies. Future work will consider the participation of variable RE sources in conventional forward markets, where participants bid to schedule energy transactions for day ahead and becomes binding once the market is cleared, then ES will play a more prominent role in the firming of RE contracts. In this case, ES could be located near wind farms or PV plant sites to taper off financial penalties associated with contract shortfalls.

VI. REFERENCES

- [1] A. Keane, L. F. Ochoa, E. Vittal, C. J. Dent, and G. P. Harrison, "Enhanced utilization of voltage control resources with distributed generation," *Power Systems, IEEE Transactions on*, vol. 26, pp. 252-260, 2011.
- [2] Y. Noorollahi, H. Yousefi, and M. Mohammadi, "Multi-criteria decision support system for wind farm site selection using GIS," *Sustainable Energy Technologies and Assessments*, vol. 13, pp. 38-50, 2016.
- [3] JO. Petinrin, M Shaaban, "The Impact of Renewable Generations on Voltage Stability in the Distribution Systems," *Renewable and Sustainable Energy Reviews*, 2016.
- [4] G. Carpinelli, G. Celli, F. Pilo, A. Russo, "Distributed generation siting and sizing under uncertainty," in *Power Tech Proceedings, 2001 IEEE Porto, 2001*, p. 7 pp. vol. 4.
- [5] R. Aghatehrani and A. Golnas, "Reactive power control of photovoltaic systems based on the voltage sensitivity analysis," in *Power and Energy Society General Meeting, 2012 IEEE, 2012*, pp. 1-5.

- [6] O. Homaei, A. Zakariazadeh, and S. Jadid, "Real-time voltage control algorithm with switched capacitors in smart distribution system in presence of renewable generations," *International Journal of Electrical Power & Energy Systems*, vol. 54, pp. 187-197, 2014.
- [7] C. W. Taylor, *Power system voltage stability*: McGraw-Hill, 1994.
- [8] M. Shaaban and J. Petinrin, "Integration of Energy Storage for Voltage Support in Distribution Systems with PV Generation," *Journal of Electrical Engineering & Technology*, vol. 11, pp. 1077-1083, 2016.
- [9] R.-H. Liang and C.-K. Cheng, "Dispatch of main transformer ULTC and capacitors in a distribution system," *Power Delivery, IEEE Transactions on*, vol. 16, pp. 625-630, 2001.
- [10] K.-S. Jeong, H.-C. Lee, Y.-S. Baek, and J.-H. Park, "Coordinated Voltage and Reactive Power Control Strategy with Distributed Generator for Improving the Operational Efficiency," *Journal of Electrical Engineering & Technology*, vol. 8, pp. 1261-1268, 2013.
- [11] Y. Liu, P. Zhang, and X. Qiu, "Optimal volt/var control in distribution systems," *International journal of electrical power & energy systems*, vol. 24, pp. 271-276, 2002.
- [12] M. Alam, K. Muttaqi, and D. Sutanto, "Distributed energy storage for mitigation of voltage-rise impact caused by rooftop solar PV," in *Power and Energy Society General Meeting, 2012 IEEE*, 2012, pp. 1-8.
- [13] X. Liu, A. Aichhorn, L. Liu, and H. Li, "Coordinated Control of Distributed Energy Storage System With Tap Changer Transformers for Voltage Rise Mitigation Under High Photovoltaic Penetration," *Smart Grid, IEEE Transactions on*, vol. 3, pp. 897-906, 2012.
- [14] A. Schroeder, "Modeling storage and demand management in power distribution grids," *Applied Energy*, vol. 88, pp. 4700-4712, 2011.
- [15] N. Khan, S. Ghosh, and S. Ghoshal, "Binary Gravitational Search based Algorithm for Optimum Siting and Sizing of DG and Shunt Capacitors in Radial Distribution Systems," *Energy and Power Engineering*, vol. 5, p. 1005, 2013.
- [16] W. S. Tan, M. Y. Hassan, H. A. Rahman, M. P. Abdullah, and F. Hussin, "Multi-distributed generation planning using hybrid particle swarm optimisation-gravitational search algorithm including voltage rise issue," *IET Generation, Transmission & Distribution*, vol. 7, pp. 929-942, 2013.
- [17] Y. M. Atwa and E. El-Saadany, "Optimal allocation of ESS in distribution systems with a high penetration of wind energy," *Power Systems, IEEE Transactions on*, vol. 25, pp. 1815-1822, 2010.
- [18] A. Zakariazadeh, O. Homaei, S. Jadid, and P. Siano, "A new approach for real time voltage control using demand response in an automated distribution system," *Applied Energy*, vol. 117, pp. 157-166, 2014.
- [19] N. Venkatesan, J. Solanki, and S. K. Solanki, "Residential Demand Response model and impact on voltage profile and losses of an electric distribution network," *Applied Energy*, vol. 96, pp. 84-91, 2012.
- [20] A.-H. Mohsenian-Rad, V. W. Wong, J. Jatskevich, R. Schober, and A. Leon-Garcia, "Autonomous demand-side management based on game-theoretic energy consumption scheduling for the future smart grid," *Smart Grid, IEEE Transactions on*, vol. 1, pp. 320-331, 2010.
- [21] Z. Zhao, W.-C. Lee, Y. Shin, and K.-B. Song, "An Optimal Power Scheduling Method for Demand Response in Home Energy Management System," *Smart Grid, IEEE Transactions on*, vol. 4, pp. 1391-1400, 2013.
- [22] J.O. Petinrin and M. Shaaban, "A voltage control scheme in a distribution feeder with wind energy sources," in *2015 IEEE Conference on Energy Conversion (CENCON)*, 2015, pp. 60-65.
- [23] R. H. Liang, Y. K. Chen, and Y. T. Chen, "Volt/Var control in a distribution system by a fuzzy optimization approach," *International Journal of Electrical Power & Energy Systems*, vol. 33, pp. 278-287, 2011.
- [24] O. I. Elgerd, *Electric energy systems theory: an introduction*: Tata McGraw-Hill Education, 1983.
- [25] J. L. Cohon, *Multiobjective programming and planning*: Courier Dover Publications, 2013.
- [26] S. Mirjalili, G.-G. Wang, and L. d. S. Coelho, "Binary optimization using hybrid particle swarm optimization and gravitational search algorithm," *Neural Computing and Applications*, pp. 1-13, 2014.
- [27] A. Ulinuha, M. A. Masoum, and S. M. Islam, "Optimal scheduling of LTC and shunt capacitors in large distorted distribution systems using evolutionary-based algorithms," *Power Delivery, IEEE Transactions on*, vol. 23, pp. 434-441, 2008.
- [28] L. Monitoring Analytics, "State of the Market Report for PJM: January through September. Technical report," *PJM Interconnection*, p. 102, 2013.